

Mechanical properties of spray-atomized Fe-40at.%Al alloys

M. Amaya, J.M. Romero, L. Martínez and R. Perez

Abstract-The room-temperature mechanical properties of intermetallic Fe-40at.% Al based alloys fabricated by spray atomization and deposition are studied. The Fe-40at.%Al, Fe-40Al+0.1at.%B, and Fe-40Al+0.1at.%B+10at.%Al₂O₃, alloys were deformed by compression under strain rates from 10⁻⁴ to 10⁻² s⁻¹. All three alloys diminished their yield stress in the interval of strain rates of 10⁻⁴-10⁻³ s⁻¹ but in the interval of 10⁻³-10⁻² s⁻¹, the Fe-40at.%Al and Fe-40Al+0.1at.%B alloys increased their yield stress. Contrary to the two last alloys the Fe-40Al+0.1at.%B+10at.%Al₂O₃ alloy shows a decrease on the yield stress in the interval of the 10⁻³-10⁻² s⁻¹. The yield stress is discussed in terms of the effect of the boron and alumina particles.

Index Terms: Intermetallic, Mechanical properties, Rapid solidification, Yield phenomena.

1.INTRODUCTION

The iron aluminides have been shown superior properties compared to the commercial alloys used in high temperature and corrosive environments [1-3]. However, the lack of ductility at room temperature has been limiting its processing and applications [4-5]. During the last decade novel processing routes, microalloying, microstructure control, particulate dispersing and fiber reinforcement have been explored to improve ductility on the iron aluminides [6-7]. Extensive studies on mechanical properties of iron aluminides have been carried out in the past [8-10], including interesting microstructure and mechanical aspects [11-20]. In the present study the spray atomization and deposited metallurgical route were explored in order to obtain FeAl intermetallic alloys doped with boron and reinforced with alumina particulate. The as-atomized mechanical properties at room temperature were evaluated and the effect of the boron and alumina particulate on the stress and strain behavior was discussed. Also, the fracture properties were analyzed. Mechanical properties at 800°C and 900°C also are reported.

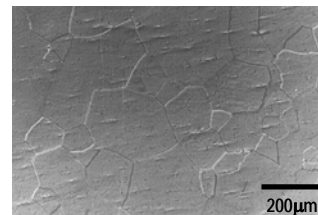
2.MATERIALS AND METHODS

Three different ingots of FeAl intermetallic alloys were fabricated by spray-atomization and deposition technique. The fabrication details are discussed elsewhere [21]. The final composition of the alloys were Fe-40at.%Al, Fe-40Al+0.1at.%B, and Fe-40Al+0.1at.%B+10at.%Al₂O₃. Several as-atomized specimens with dimensions of 10x5x5 mm were obtained from the ingots using a spark cutting machine. The specimens were cut following the spray-atomization direction. A face of each parallelepiped specimens were mechanical grinding with wet SiC-paper (grit 600). Finally the specimens were polished using

colloidal alumina of 3 and 1 μm. Then the polished faces were etched with a solution of 33% nitric acid, 33% acetic acid, 33% H₂O and 1% fluorhydric acid (volume %). The intercept method (ASTM-E112) was employed to measure the grain sizes. Before the compression tests all parallelepiped specimens were mechanical grinding with wet SiC-paper (grit 600) and subsequently polished using colloidal alumina of 3 and 1 μm. Compressive mechanical tests were carried out at room temperature using an universal testing machine (Instron 4206), at strain rates (SR) of 10⁻⁴, 10⁻³, and 10⁻² s⁻¹. A Teflon film was used to minimize the friction between specimens and the compression pads. The FeAl specimens were strained to failure. The yield stresses were measured at 0.2% plastic strain (0.2% offset yield strength). After compression tests all fracture surfaces of the specimens were examined by a JEOL 400 Scanning electron microscopic. Compressive mechanical tests at 800°C and 900°C with a strain rate of 10⁻³ s⁻¹ were performed. SiN bearing blocks lubricated with graphite were used between specimens and compression pads to minimize the friction.

3.RESULTS

The Fe-40at.%Al and Fe-40Al+0.1at.%B alloys (Figure 1a and 1b, respectively)



(a)

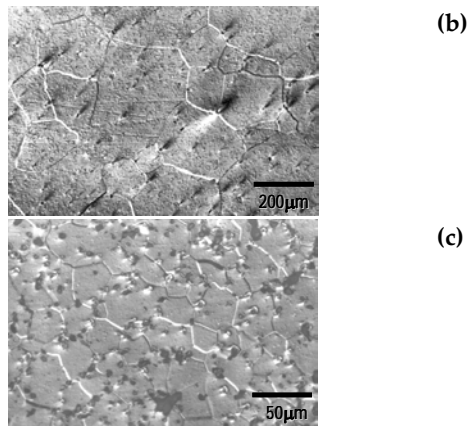


Figure 1. As-atomized microstructures of the (a) Fe-40at.%Al, (b) Fe-40Al+0.1at.%B, and (c) Fe-40Al+0.1at.%B+10at.%Al₂O₃ intermetallic alloys.

showed non-uniform initial grain sizedistribution in its as-atomized condition compared to the Fe-40Al+0.1at.%B+10at.%Al₂O₃ alloy (Figure 1c). The presence of Al₂O₃ particulate induced a grain size refinement and improves the microstructure of the Fe-40Al+0.1at.%B+10at.%Al₂O₃ alloy.

The average grain size of the specimens were 80, 147, and 65 μm for the Fe-40at.%Al, Fe-40Al+0.1at.%B, and Fe-40Al+0.1at.%B+10at.%Al₂O₃ alloys, respectively. The true stress-strain curves of the FeAl base alloys are shown in the figures 2, 3 and 4, respectively. These curves show that the all three alloys yield continuously and smoothly. In the past, several researches have reported that the fine-grained FeAl alloys yields discontinuously while

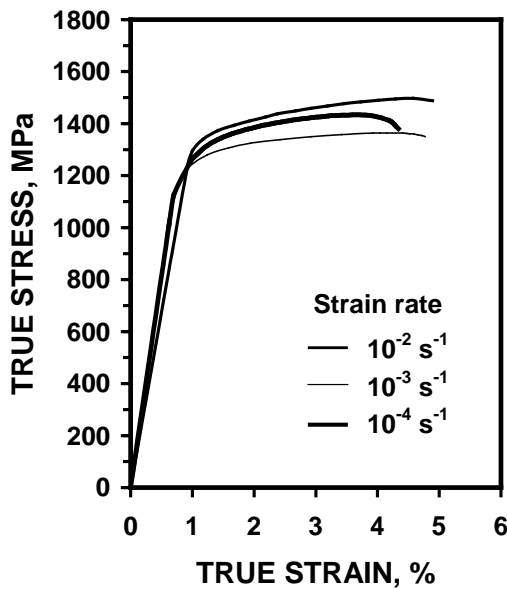


Figure 2. Compressive stress-strain curves of the Fe-40at.%Al alloy.

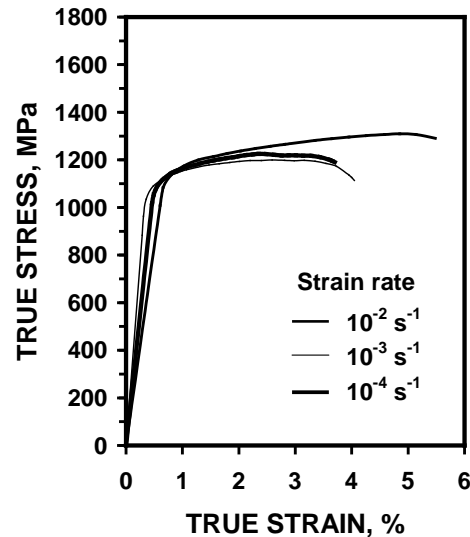


Figure 3. Compressive stress-strain curves of the Fe-40Al+0.1at.%B alloy.

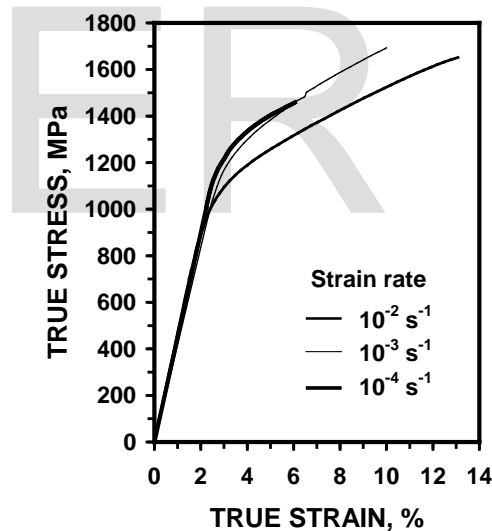


Figure 4. Compressive stress-strain curves of the Fe-40Al+0.1at.%B+10at.%Al₂O₃ alloy.

large-grained yields smoothly [11,13,18,22]. In the Fe-40at.%Al and Fe-40Al+0.1at.%B alloys the ultimate strength (US) raises constantly as the strain rate diminishes. However in the Fe-40Al+0.1at.%B+10at.%Al₂O₃ alloy, the US increases abruptly in the SR range from 10⁻² to 10⁻³ s⁻¹. The US remaining cuasiconstantly in the SR of 10⁻³ s⁻¹ and 10⁻⁴ s⁻¹. The figure 5 shows the effect of the SR on the 0.2% offset yield strength (YS). In the SR range of 10⁻² to 10⁻³ s⁻¹, the Fe-40at.%Al and Fe-

40Al+0.1at.%B alloys diminished the YS and then, the YS increases up to SR of 10^{-4} s^{-1} . Also, the figure 5 shows that the boron diminished the YS compared as the YS of the FeAl40at% base alloy, about 150 MPa.

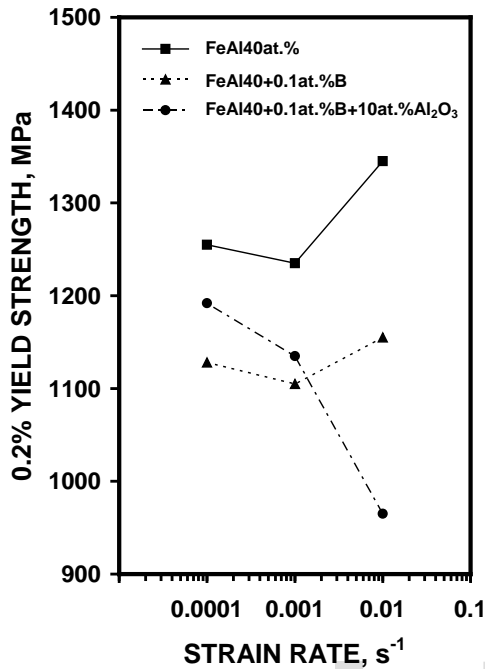


Figure 5. Effect of the strain rate on the 0.2% yield strength at room-temperature.

The effect of the SR on the YS is shown in the figure 5. Basically, the Fe-40at%Al and Fe-40Al+0.1at%B alloys showed a similar performance. The YS diminished as the strain rate diminished from 10^{-2} to 10^{-3} s^{-1} , then, the YS increased as the strain rate increased from 10^{-3} to 10^{-4} s^{-1} . On the other hand, in the Fe-40Al+0.1at%B+10at%Al₂O₃ alloy the YS increased constantly, as the strain rate increased from 10^{-2} to 10^{-4} s^{-1} .

Figure 6 shows the effect of the strain rate on the final strain before the rupture in the all three FeAl alloys. The Fe-40at.%Al alloy increased the strain smoothly as the strain rate diminished. On the other hand, the FeAl40+0.1at%B and

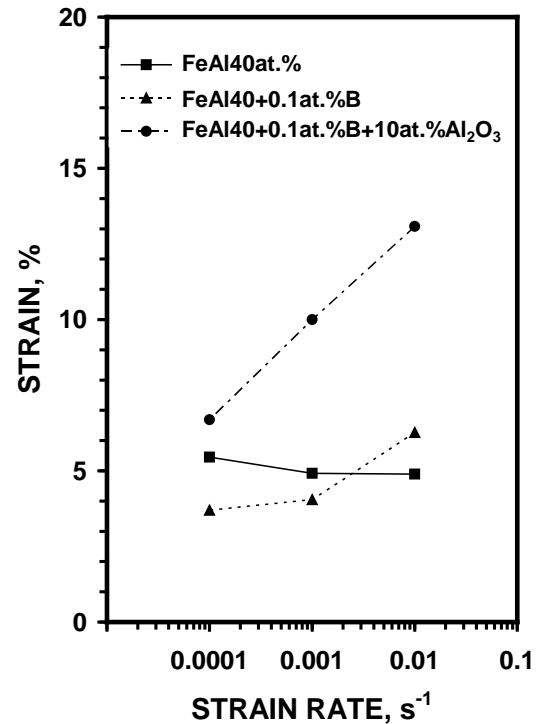
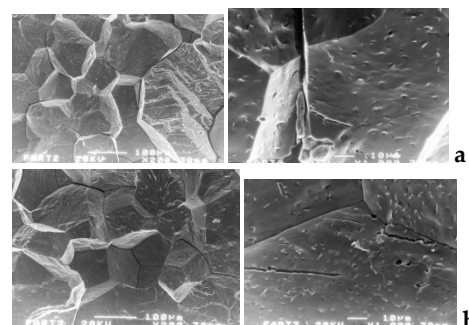


Figure 6.

Graph of strain as a function of the strain rate.

Fe-40Al+0.1at%B+10at%Al₂O₃ alloys diminished the strain as the strain rate diminished. Compared as the Fe-40Al+0.1at%B alloy the percentage of strain in the Fe-40Al+0.1at%B+10at%Al₂O₃ alloy diminished abruptly. The Al₂O₃ particulate detachment could generate the last effect because these particles promote crack niches before the plastic deformation can occurred during the deformation.

This effect is promoted by the disbondement of the alumina particles, which are the sites for the crack initiation inducing material failures before the plastic deformation. The B presence affects the deformation nature of the Fe-40Al+0.1at%B and Fe-40Al+0.1at%B+10at%Al₂O₃ alloys. The deformation percentage gets lower with the dismition of the strain rate in the Fe-40Al+0.1at%B and Fe-40Al+0.1at%B+10at%Al₂O₃ in comparison with Fe-40at.%Al.



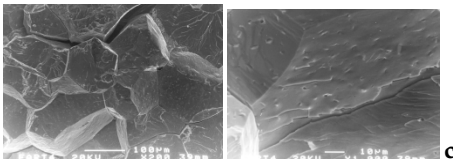


Figure 7. Fractographies of the Fe-40at.%Al alloy after the compression tests at strain rates of (a) 10^{-2} s^{-1} , (b) 10^{-3} s^{-1} , and (c) 10^{-4} s^{-1} .

In the figure 7, the fracture surfaces obtained in the Fe-40at.%Al alloy are presented. We can see in the figure 7b which corresponds to test condition of 10^{-3} s^{-1} the fracture surface shows more microcleavage cracks density compared with the other two strain rates. The formation of microcleavage cracks caused by this strain rate can be contributed to drop the yield stress. On the other hand, the drop of yield stress in the Fe-40Al+0.1at.%B alloy can be attributed at different factors. In this case, the pores seem to play an important role because they incubate and transmit cracks paths (figure 7b) that contributed to lower the microstructural integrity.

Figure 5 also shows a difference of yield stress between Fe-40at.%Al and Fe-40Al+0.1at.%B alloys. Others researchers have found that the boron segregates at the grain boundaries improving the cohesion, and suppressing the intergranular fracture [5,23]. In the present study the pores formed in the microstructure of the Fe-40Al+0.1at.%B alloy (see figure 7) can affect the boron distribution in the microstructure. Although, no evidence was found of boron distribution. We believe that part of boron can be segregated in the free surface of the pores, obscuring the beneficial effect on the grain boundaries.

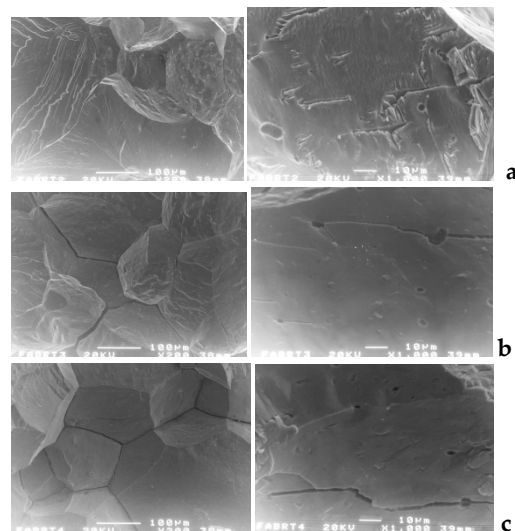


Figure 8. Fractographies of the Fe-40Al+0.1at.%B alloy after the compression tests at strain rates of (a) 10^{-2} s^{-1} , (b) 10^{-3} s^{-1} , and (c) 10^{-4} s^{-1} .

In the Fe-40Al+0.1at.%B+10at.%Al₂O₃ alloy the yield stress gets

lower values consistently with the increase of the strain rate. This behavior was attributed to the generation of cracks in the grain boundaries which is promoted by the alumine particles. The figure 8 shows evidence of cracks and alumina particulate on the grain boundaries. On the other hand, it seems that the strain rate play an important role in the strenght of this alloy as is illustrated in figure 5.

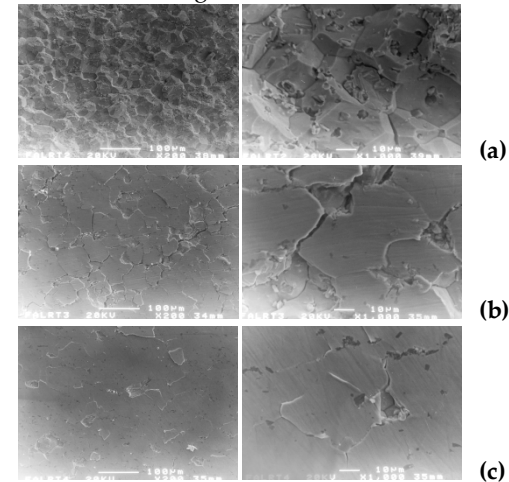


Figure 9. Fractographies of the Fe-40Al+0.1at.%B+10at.%Al₂O₃ alloy after the compression tests at strain rates of (a) 10^{-2} s^{-1} , (b) 10^{-3} s^{-1} , and (c) 10^{-4} s^{-1} .

These figures illustrate evidence of cracks along the grain boundaries, figures 9a and 9b, however at the lowest strain rate (10^{-4} s^{-1}), less crack density is found.

Finally, figure 10 shows the effects of the temperature on the 0.2% yield strength. At 800°C, the 0.2% yield

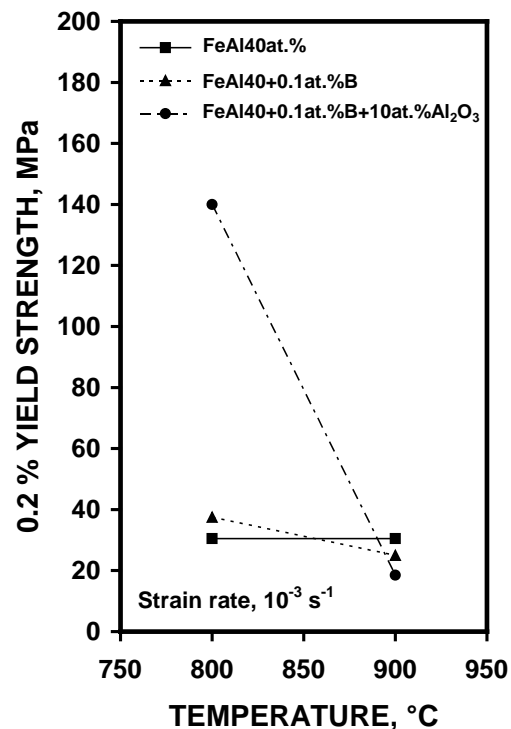


Figure 10.

Effect of the temperature on the 0.2% yield strength.

strength is 100 MPa larger than in the Fe-40Al+0.1at%B+10at%Al₂O₃ alloy in comparison with the Fe-40Al+0.1at%B and Fe-40at.%Al alloys. However, at 900°C, these effects are not observed and the FeAl40at% alloy has better mechanical behavior than the Fe-40Al+0.1at%B and the Fe-40Al+0.1at%B+10at%Al₂O₃ alloys.

4. CONCLUSIONS

The room-temperature mechanical behavior of intermetallic Fe-40at.%Al based alloys fabricated by spray atomization and deposition were studied. All alloys yield continuously in the strain rate interval of 10⁻⁴ to 10⁻² s⁻¹. The Fe-40at.%Al and Fe-40Al+0.1at.%B alloys showed a diminishing in the yield stress at strain rates of 10⁻³ s⁻¹. This behavior was attributed to high density of microcleavage in the Fe-40at.%Al, and in the Fe-40Al+0.1at.%B it was related to cracks induced by pores that lowers the microstructural integrity. On the other hand, in the Fe-40Al+0.1at.%B+10at.%Al₂O₃ alloy the yield stress diminished consistently with increase of the strain rate. We found evidence that alumina particles play an important role in the drop of yield stress because they promote cracks that degrade the mechanical properties.

ACKNOWLEDGEMENTS

The authors acknowledge the SEM technical support of O. Flores.

REFERENCES

[1]. Yoo M. H., Horton J. A., and Liu C. T., Micromechanisms of yield and flow in ordered intermetallic alloys., *Acta metall.*, 1988; **36**, 2935.
[2]. Sikka V. K. in *Processing, Properties and Applications of Iron Aluminides*, TMS, Warrendale PA, 1994; p. 3.
[3]. Amaya M., PHD Thesis, Universidad Nacional Autonoma de Mexico, 1999.
[4]. Liu C. T. and McKamey C in *High Temperature Aluminides and Intermetallics*, TMS, Warrendale PA, 1990; p. 133.
[5]. Liu C. T. and George E. P., Environmental embrittlement in boron-free and boron-doped Fe-Al (40 at.%Al) alloys., *Scripta Metallurgica et Materialia*, 1990; **24**, 1285.
[6]. Baker I. and Munroe P. R., Mechanical properties of FeAl., *International Materials Reviews*, 1997; **42**, 181.
[7]. Martinez L., Amaya M., Porcayo-Calderon J., Lavernia E. J., High temperatura electrochemical testing of spray atomized and deposited iron aluminides alloyed with boron and reinforced with alumina particulate., *Mater. Sci. Eng.*, 1998; **A258**, 306.
[8]. Whittenberger J. D., Influence of thermomechanical processing on elevated temperature slow plastic flow properties of B2 aluminide Fe-39.8 at%Al., *Mater. Sci. Engng.*, 1983; **57**, 77.
[9]. Baker I. and Gaydosh D. J., Flow and fracture of Fe-Al., *Mater. Sci. Engng.*, 1987; **96**, 147.
[10]. Schmidt B., Nagpal P., and Baker I., *Mat. Res. Soc. Symp. Proc.*, 1989; **133**, 755.

[11]. Baker I., Nagpal P., Liu F., and Munroe P. R., The effect of grain size on the yield strength of FeAl and NiAl., *Acta metall. Mater*, 1991; **39**, 1637.
[12]. Pike L. M. and Liu C. T., The effect of boron doping in the hall-petch slope of FeAl (40at.%Al)., *Scripta Metallurgica et Materialia*, 1991; **25**, 2757.
[13]. Gaydosh D. J., Draper S. L., Noebe R. D., and Nathal M. V., Room temperature flow and fracture of Fe-40at.%Al alloys., *Mater. Sci. Engng.*, 1992; **A150**, 7.
[14]. Baker I., Klein O., Nelson C., and George E. P., Effects of boron and grain size on the strain-rate sensitivity of Fe-45Al., *Scripta Metallurgica et Materialia*, 1994; **30**, 863.
[15]. Baker I. Xiao, H., Klein O., Nelson C., and Whittenberger J., The effect of temperature and Fe:Al ratio on the flow and fracture of FeAl., *Acta metall. Mater*, 1995; **43**, 1723.
[16]. Imayev R., Evangelista E., Tassa O., Stobrawa J., Relationships between mechanism of deformation and development of dynamic recrystallization in FeAl intermetallic., *Mater. Sci. Engng.*, 1995; **A202**, 128.
[17]. Scheff S. A., Stout J. J., and Crimp M. A, Effects of extraction texture on the compressive behavior of B2 FeAl alloys., *Scripta Metallurgica et Materialia*, 1995; **32**, 975.
[18]. Morris D. G., Gunther S., Strength and ductility of Fe-40Al alloy prepared by mechanical alloying., *Mater. Sci. Eng.*, 1996; **A208**, 7.
[19]. Baker I. and Yang Y., On the yield stress anomaly in stoichiometric FeAl., *Mater. Sci. Engng.*, 1997; **A239-240**, 109.
[20]. Cohron J. W., Lin Y., Zee R., and George E. P., Room temperature mechanical behavior of FeAl: effects of stoichiometry, environment and boron additions., *Acta mater* 1998; **46**, 6245.
[21]. Martinez L., Flores O., Amaya M., Duncan A., Viswanathan S, Lawrynowics D., and Lavernia E. J., The role of alumina particulate in microstructural and forging properties of spray atomized and deposited Fe-Al ordered intermetallic compounds., *Journal of Materials Synthesis and Processing*, 1997; **5**, 65.
[22]. Briguet C. and Morris D. G., Deformation mechanics in a mechanically alloyed Fe-40Al alloy and the influence of recrystallization and ageing heat treatments., *Acta mater*, 1997; **45**, 4939.
[23]. Crimp M. A and Vedula K. M., Effect of boron on the tensile properties of B2 FeAl., *Mater. Sci. Eng.*, 1986; **78**, 193.